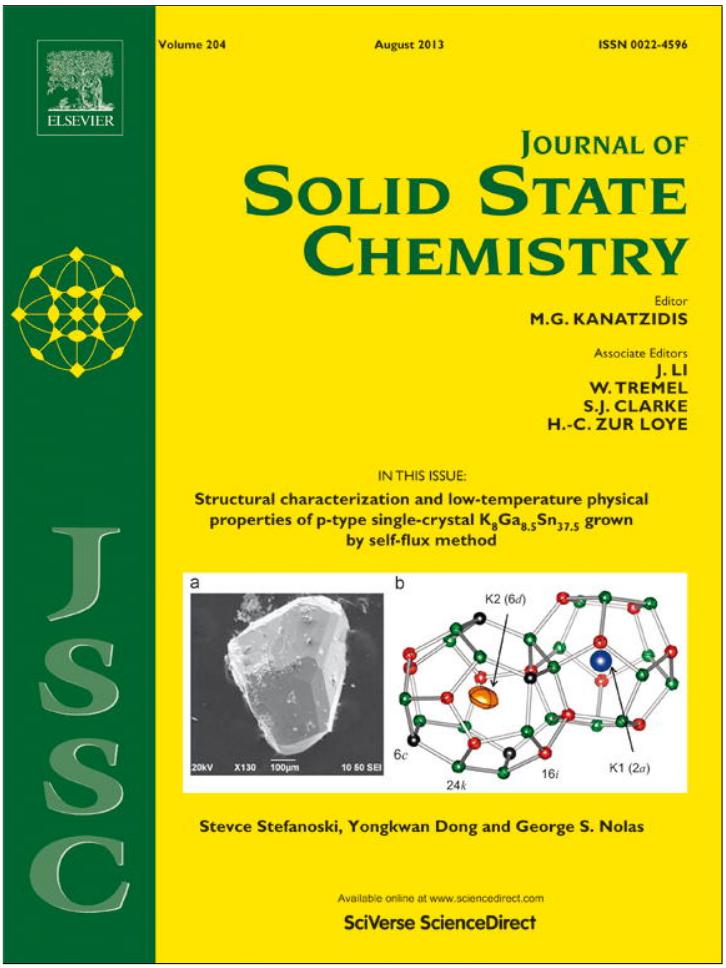

Journal of Solid State Chemistry 204 (2013) 190–196

Contents lists available at SciVerse ScienceDirect

Journal of Solid State Chemistry

journal homepage: www.elsevier.com/locate/jssc

Two new coordination polymers constructed by naphthalene-1,4-dicarboxylic acid and 2,4-diamino-6-methyl-triazine

Yamin Li [a,*], Changyu Xiao [a], Xudong Zhang [b], Yanhui Xu [c], Junrui Li [a], Huijie Lun [a], Qi Chen [a]

[a] Institute of Molecular and Crystal Engineering, College of Chemistry and Chemical Engineering, Henan University, Kaifeng, Henan 475004, PR China
[b] State Key Laboratory of Structural Chemistry, Fujian Institute of Research on the Structure of Matter, Chinese Academy of Sciences, Fuzhou, Fujian 350002, PR China
[c] Department of Medical Imaging, Bethune Medical Non-Commissioned Officer's, College, Shijiazhuang, Hebei 050081, PR China

ARTICLE INFO

Article history:
Received 13 March 2013
Received in revised form
21 May 2013
Accepted 21 May 2013
Available online 29 May 2013

Keywords:
Decanuclear silver units
Topology
Photoluminescent property
Magnetic property

ABSTRACT

Two new transition metal coordination complexes, $\{[MnO(nda)](H_2dmt)(H_2O)\}_n$ (**1**), $[Ag_5(nda)_{2.5}(dmt)]_n$ (**2**), (H_2nda=naphthalene-1,4-dicarboxylic acid, dmt=2,4-diamine-6-methyl-1,3,5-triazine) have been hydrothermally synthesized by the reactions of H_2nda and dmt with the homologous $MnCl_2 \cdot 4H_2O$ and $AgNO_3$, respectively, and characterized by single-crystal X-ray diffraction, IR spectra, elemental analysis, thermogravimetric analysis (TGA). The compound **1** exhibits a 3D network comprising 1D metal chain $\{MnO(CO_2)_2\}_n$ connected by the ligand nda^{2-}, featuring a four-connected uninodal diamond -like topology. In compound **2**, it is firstly observed that decanuclear silver units as secondary building units to construct 3D network by the ligands dmt and nda^{2-}, with a rare 2-nodal (3,8)-connected **tfz-d** topology ($\{4^3\}_2\{4^6.6^{18}.8^4\}$). The interactions within each Mn(II)—Mn(II) pair of compound **1** are antiferromagnetic (g=2.07, J=−1.42(1) cm^{-1}, zj'=−0.73(2) cm^{-1}). In addition, compound **2** exhibits photoluminescent property at about 472 nm (λ_{ex}=394 nm).

1. Introduction

Recently, the design and construction of polynuclear transition metal coordination polymers have attracted a great deal of interest in the field of supramolecular chemistry and crystal engineering, not only due to their fascinating architectures and molecular topologies, but also for their potential applications in magnetism [1–3], optical properties [4,5], gas storage/ separation [6,7], catalysis [8], and so on. From the synthetic point of view, the smart selection of appropriate organic ligand is proved to be an effective way to synthesize the versatile transition metal coordination polymers. Among multitudinous organic ligands, aromatic carboxylic acids, particularly, which can coordinate to transition metal ions through different carboxylato-bridging modes (*syn–syn*, *anti–anti*, *syn–anti*), have been proven to be good candidates [9–12]. As well, this kind of ligands contains rigid configurations, which is difficult to change the spatial orientations between coordinating dentates during the coordinations, so it is easy to control to obtain the objective products. On the other hand, the auxiliary ligands with N-containing groups are introduced to the carboxylate systems for the construction of polymeric frameworks. The 2,4-diamine-6-methyl-1,3,5-triazine (dmt) is a potentially versatile *N*-heterocyclic ligand which contains three coordinating N-atoms with 120° angles and may act as a three-connected node. The presence of $-NH_2$ of dmt can also form hydrogen bonding interactions with either carboxyl-O atoms or nitrogen atoms or solvent molecules [13,14]. Moreover, the aromatic rings from dmt and aromatic carboxylic acid are capable to form $\pi\cdots\pi$ stacking interactions, which play an important role in the formation of packing structure. Although fascinating architectures and properties of transition metal coordination complexes with aromatic carboxylic acid/ N-containing ligands have been widely investigated, to the best of our knowledge, only limited compounds containing M-dmt have been documented to date [15,16].

Herein, based on the self-assembly of H_2nda and dmt with different transition metal salts ($MnCl_2 \cdot 4H_2O$ or $AgNO_3$), two new coordination polymers, $\{[MnO(nda)](H_2dmt)(H_2O)\}_n$ (1) and $[Ag_5(nda)_{2.5}(dmt)_2]_n$ (2) (H_2nda=naphthalene-1,4-dicarboxylic acid, dmt=2,4-diamine-6-methyl-1,3,5-triazine), have been achieved. The compound 1 exhibits a 3D network consisting of 1D linear chains $\{MnO(CO_2)_2\}_n$ connected by the ligands nda^{2-}, which features a four-connected uninodal diamond-like topology. For compound **2**, it is firstly observed that the 3D network is built up by decanuclear silver units as secondary building units connected by the ligands dmt and nda^{2-}, which exhibits a rare 2-nodal (3,8)-connected **tfz-d** topology ($\{4^3\}_2\{4^6.6^{18}.8^4\}$). As far as we know, only one case **tfz-d** topology has been reported [17]. The magnetic measurement indicates the compound **1** is antiferromagnetic. In

* Corresponding author. Fax: +86 378 3881589.
E-mail address: liyamin@henu.edu.cn (Y. Li).

0022-4596/$ - see front matter © 2013 Elsevier Inc. All rights reserved.
http://dx.doi.org/10.1016/j.jssc.2013.05.028

addition, compound **2** exhibits photoluminescence in the solid state at room temperature.

2. Experimental

2.1. Materials and methods

All materials were commercially available and used as received. Infrared spectra were recorded on a Nicolet magna 750 FT-IR spectrophotometer using KBr pellets in the range of 400∼4000 cm^{-1}. Elemental analyses were performed *via* Vario EL III Etro Elemental Analyzer. Thermogravimetric analyses (TGA) were performed under atmosphere with a heating rate of 10 °C/min using TGA/SDTA851e. Photoluminescence spectra were measured on a Hitachi Fluorescence spectrophotometer—F-7000. Magnetic measurements were carried out on a Quantum Design MPMS-XL SQUID magnetometer, and diamagnetic corrections were estimated from Pascal's constants.

2.2. Syntheses of the complexes

2.2.1. Synthesis of {[MnO(nda)](H2dmt)(H2O)}n (1)

H_2nda (0.216 g, 1 mmol), dmt (0.125 g, 1 mmol) and $MnCl_2 \cdot 4H_2O$ (0.394 g, 2 mmol) in 10 mL of H_2O were stirred for 20 min at room temperature, and the mixture was sealed in a 25 mL Teflon-lined reactor, which was heated to 150 °C for 3 days. After the autoclave had been cooled to room temperature over 6–7 h, yellow strip crystals of **1** were obtained, and washed by H_2O (Yield: 0.180 g, 41.8% based on H_2nda). Anal. Calc. for (%): $C_{16}H_{17}MnN_5O_6$: C 44.65, H 3.98, N 16.28; Found: C 44.54, H 3.92, N 16.31. IR (KBr, pellet, cm^{-1}): 3429m, 3174s, 2359 w, 1653m, 1557s, 1512m, 1458m, 1410m, 1364s, 1264m, 1208m, 1162w, 829m, 793m, 776m, 625w.

2.2.2. Synthesis of [Ag5(nda)2.5(dmt)]n (2)

Replacement of $MnCl_2 \cdot 4H_2O$ of **1** by $AgNO_3$ (0.340 g, 2 mmol), brown block crystals of **2** were obtained (Yield 0.194 g, 40.4% based on H_2nda). Anal. Calc. for (%), C 34.03, H 1.85, N 5.84; Found: C 34.08, H 1.78, N 5.76. IR (KBr pellet, cm^{-1}): 3429m, 2361m, 1663s,1556s, 1458m, 1411s, 1365s, 1261m, 1212m, 1162w, 1016m, 801m, 668w.

2.2.3. Crystallographic data collection and refinement

X-ray single crystal data of the compounds **1** and **2** were collected at 296 (2) K on a Bruker Apex-II CCD area detector diffractometer with Mo*K*α radiation (λ=0.71073 Å). Data reduction and absorption correction were made with empirical methods. These structures were solved by direct methods using SHELXS-97 [18] and refined by full matrix least-squares methods using SHELXL-97 [19]. Anisotropic displacement parameters were refined for all non-hydrogen atoms; and all hydrogen atoms bonded to carbon and nitrogen atoms were added in the riding model while the aqueous hydrogen atoms of **1** were located from the difference Fourier maps. The crystal data and refinement details for two complexes are listed in Table 1.

Table 1
Crystal data and refinement details of the compounds **1–2**.

	1	**2**
Empirical formula	$C_{16}H_{17}MnN_5O_6$	$C_{34}H_{21}Ag_5N_5O_{10}$
Formula mass [g mol^{-1}]	430.29	1198.91
Crystal size [mm]	0.45 × 0.14 × 0.11	0.36 × 0.22 × 0.18
Space group	*P*2(1)/*n*	*C*2/*c*
a [Å]	7.512(10)	31.088(4)
b [Å]	16.53(2)	11.2507(13)
c [Å]	14.154(17)	19.208(2)
α [°]	90	90
β [°]	90.17(2)	92.060(2)
γ [°]	90	90
V [$Å^3$]	1757(4)	6714.0(13)
Z	4	8
μ [mm^{-1}]	0.798	2.372
ρ calcd. [g cm^{-3}]	1.626	2.934
θ limits [°]	1.89 to 25.00	1.93 to 25.00
h limits	−8 to 8	−35 to 36
k limits	−19 to 16	−13 to 8
l limits	−16 to 9	−22 to 21
Collected reflections	7212	13870
Independent reflections (R_{int})	3084(0.0401)	5792(0.0185)
R index [obs.]	R_1 =0.0522	R_1 =0.0489
	wR_2=0.1408	wR_2=0.1013
R (all data)	R_1 =0.0777	R_1 =0.0530
	wR_2=0.1604	wR_2=0.1026
GOOF	1.077	1.293
$\Delta\rho_{min}$ [e$Å^{-3}$]	−0.861	−1.321
$\Delta\rho_{max}$ [e$Å^{-3}$]	0.559	1.782

[a] $R=\sum(||F_o|-|F_c||)/\sum|F_o|$, [b] $wR=\{\sum w[(F_o^2-F_c^2)^2]/\sum w[(F_o^2)^2]\}^{1/2}$, $w=1/[\sigma^2(F_o^2)+(aP)^2+bP]$, $P=(F_o^2+2F_c^2)/3$]. **1**, a =0.0652, b=2.4166; **2**, a=0.0202, b=92.8748.

3. Results and discussion

3.1. Synthesis and IR spectroscopy

The hydrothermal reaction of H_2nda, dmt and $MnCl_2 \cdot 4H_2O$ (or $AgNO_3$) at 1:1:2 ratio gave rise to the coordination polymer **1** (or **2**). However, under the same conditions, we made an attempt to prepare other crystals by using other transition metal salts such as $ZnCl_2$, $CdCl_2 \cdot 2.5H_2O$ or $CuCl_2 \cdot 2H_2O$ as the materials, but the only precipitates were obtained without further analyses. It is inferred that the conditions such as the pH value or reacting temperature might be not suitable for crystallization of other compounds.

The IR spectra show the peaks at 3430 cm^{-1} for **1** (3429 cm^{-1} for **2**) should be ascribed to $-NH_2$ stretching vibrations, demonstrating the presence of dmt in two compounds. The asymmetric stretching vibrations of carboxylic groups are assigned to the 1557 cm^{-1} for **1**, 1663 and 1566 cm^{-1} for **2**, while the symmetric stretching vibrations at 1364 cm^{-1} for **1**, 1411 and 1365 cm^{-1} for **2**, respectively, which indicate the carboxylic groups coordinating to the metal atoms in bridging fashion [20].

3.2. Crystal structure of complex 1

The complex **1** crystallizes in monoclinic group *P*2(1)/*n*, showing a 3D network by 1D linear chain $\{MnO(CO_2)_2\}_n$ connected by the ligand nda^{2-}. As shown in Fig. 1, there exist two half Mn(II) ions: one nda^{2-}, one μ_2-O atom, one H_2dmt cation and one free water molecule in the asymmetric unit of **1**. The crystallographically independent Mn1 and Mn2 with both 1/2 site occupancies have elongated octahedral arrangement in [MnO_6], of which four equatorial oxygen atoms from four different nda^{2-}, and two axial oxygen from μ_2-O atoms. A significant elongation around the two Mn(II) atoms occurs as a result of Jahn–Teller effect [21]. Two axial sites are separated from Mn(1) with 2.335(4) Å for Mn(1)–O (5) and Mn(1)–O(5A) (A: −*x*, 1−*y*, 1−*z*), longer than the equatorial Mn–O distances of 2.183(3) Å and 2.086 Å. For Mn(2), the axial distances of Mn(2)–O(5) and Mn(2)–O(5B) (B: 1−*x*, 1−*y*, 1−*z*) are 2.316(4) Å, and the equatorial Mn–O distances are almost equal, which are 2.142(3) Å and 2.141(3) Å. The Mn–O bond lengths are in agreement with the distances reported earlier of this type of coordination environment [22–25]. The coordination angles, ranging from 84.46(15) to 95.54(15) (see Table S1), are indicative of a slightly distorted octahedral geometry (the ideal angle being 90°).

As shown in Fig. 2, along *a*-axis, the adjacent Mn(II) atoms are connected to one-dimensional linear chain $\{MnO(CO_2)_2\}_n$ by two

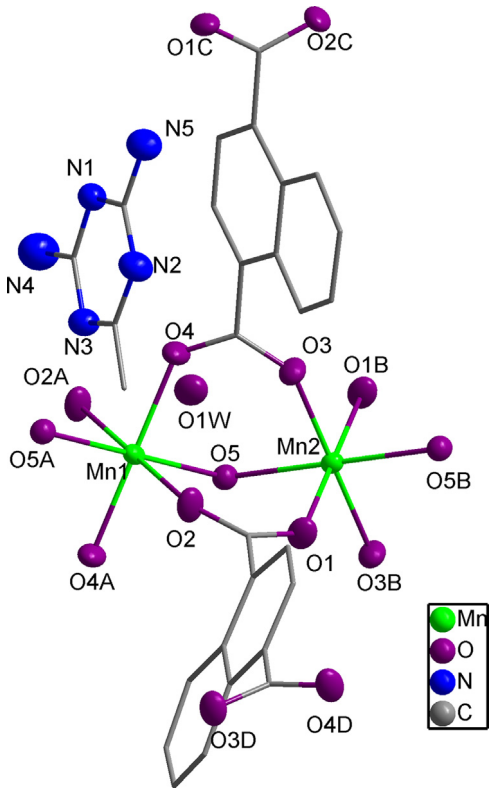

Fig. 1. The construction unit of **1** with thermal ellipsoid at 50% probability (symmetry codes: A: –*x*, 1–*y*, 1–*z*; B: 1–*x*, 1–*y*, 1–*z*; C: 0.5–*x*, 0.5+*y*, 1.5–*z*; D: 0.5–*x*, –0.5+*y*, 1.5–*z*).

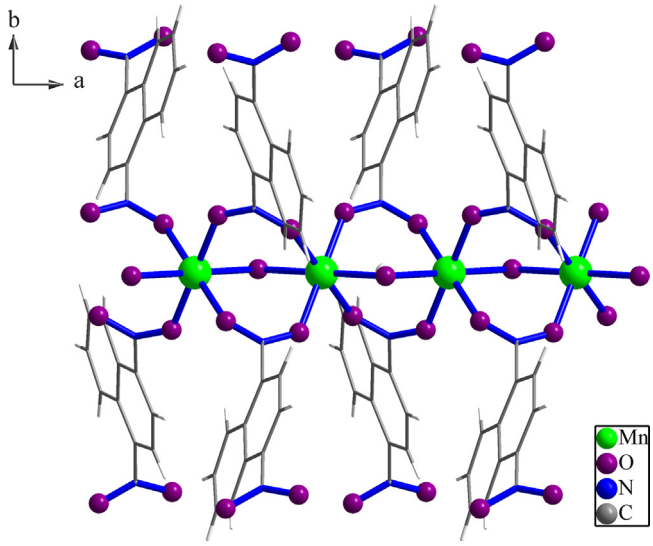

Fig. 2. The linear chain of **1** viewed perpendicular to the *c* axis.

syn, *syn*-μ_2:η^1:η^1-carboxylic oxygen atoms and one μ_2-O atom. Each chain is connected to four other chains through μ_4:η^1:η^1:η^1:η^1-nda^{2-} ligands forming a 3D network, and some 1D channels are built up with aperture approximately 3×4 Å with the cation H_2dmt^{2+} located (Fig. 3). The shortest intrachain and interchain Mn···Mn distances are 3.756 Å, 10.881 Å, respectively. From the view of topology (Fig. 4), if the adjacent Mn1 and Mn2 atoms are treated as one four-connected node and the ligand nda^{2-} is looked as linear linker, the overall structure is simplified as a uninodal four-connected 3D network, which is noted as diamond-like topology, slightly different from the reported tetrahedral nodes [26–28].

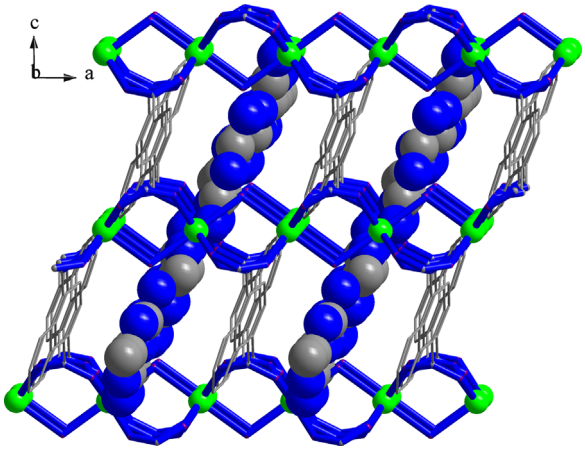

Fig. 3. View of 1D channels of **1** with the cation H_2dmt^{2+} located.

Here, each dmt obtains two hydrogen protons forming H_2dmt^{2+} ligand to balance the charge of anionic network $[MnO(nda)]^{2-}$. Though the cation H_2dmt^{2+} do not participate in coordinating to the metal ion, a kind of strong $\pi\cdots\pi$ packing interaction is observed from triazine ring and naphthyl ring between the cation H_2dmt^{2+} and nda^{2-} with the vertical plane–plane distance of 3.38 Å, the centroid–centroid distance of about 3.82 Å, as well as H_2dmt^{2+} and free H_2O molecules are involved in the formation of several hydrogen bonding interactions (see Table S2), which play an important role in stabilizing the framework.

Many compounds of H_2nda-based Mn(II) coordination polymers have been discussed in the literature; however, most of them also contain coordinating N-donor auxiliary co-ligands, which might be rare by the use of only coordinating H_2nda. In fact, the only example is the 3D compound $[Mn(1,4\text{-napdc})]_n$ (1,4-ndpdcH_2=naphthalene-1,4-dicarboxylic acid) [29], where a 1D chain of $[Mn\text{-}\mu\text{-}O_2]_n$ is also observed consisting of Mn(II) atoms and carboxylic oxygen atoms, which is different from that of **1** in that the 1D chain is built up of Mn(II) atoms, μ_2-O atom and carboxylic groups. Another difference is the coordination mode of 1,4-nda^{2-} in two compounds, which is μ_6:η^1:η^1:η^1:η^1:η^1:η^1 mode in that case and μ_4:η^1:η^1:η^1:η^1 mode in **1**.

3.3. *Crystal structure of complex **2***

When the manganese salt of **1** is replaced by silver salt, complex **2** is obtained. Complex **2** crystallizes in monoclinic *C*2/c and consists of decanuclear silver units connected to form the 3D network by the ligands dmt and nda^{2-}. From Fig. 5, the asymmetric unit of **2** contains five Ag(I) ions, two and a half nda^{2-}, one dmt. Ag1 and Ag5 atoms are bridged by two carboxylic groups from two nda^{2-} ligands. Besides, Ag1 atom is coordinated to another oxygen atom from another nda^{2-} ligand, while Ag5 is coordinated to one nitrogen atom from one dmt ligand, resulting in three-coordinated trigonal planar geometries, mean deviation from planarity of 0.0175 Å and 0.0633 Å, respectively. Ag2 and Ag3 atoms bear linear geometries by coordinated to one nitrogen atom from one dmt ligand and one oxygen atom from one nda^{2-} ligand with N–Ag–O of about 154.5(2) ° and 172.5(2) °, respectively, and Ag4 forms a trigonal planar configuration by coordinated to three carboxyl oxygen atoms with mean deviation from planarity of about 0.0481 Å. The Ag–O and Ag–N lengths ranging from 2.185 (5) to 2.444(5) Å and 2.185(6) to 2.443(6) Å (see Table S1), respectively, are corresponding to this type of coordination environments [30,31]. Besides, several additional Ag–O weak interactions are observed to connect Ag1A, Ag2, Ag3B, Ag4 and Ag5A (A: 0.5–*x*, 0.5+*y*, 0.5–*z*; B: *x*, 1+*y*, *z*) atoms into Ag_5 units with Ag–O

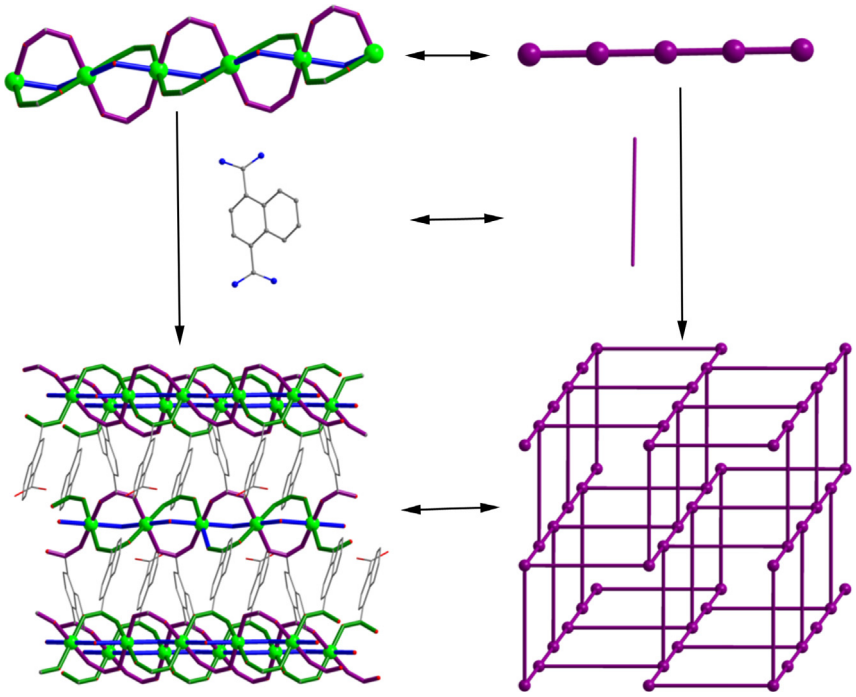

Fig. 4. View of the diamond-like topology of **1** and its schematic description.

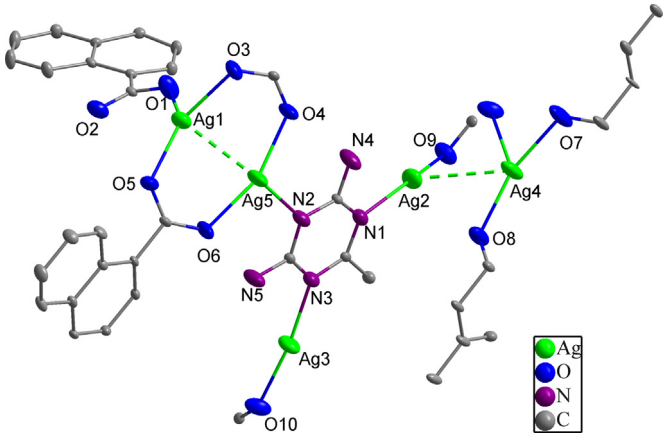

Fig. 5. The asymmetrical unit of **2** with thermal ellipsoid at 50% probability.

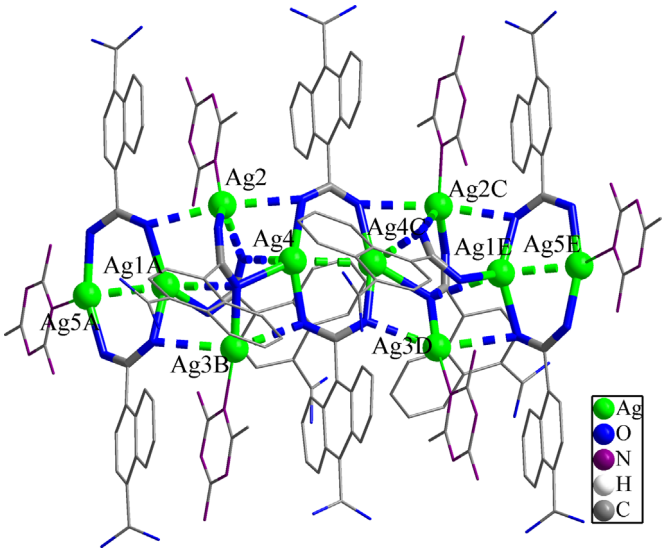

Fig. 6. Decanuclear silver unit of **2** (symmetry codes: A: 0.5–*x*, 0.5+*y*, 0.5–*z*; B: *x*, 1+*y*, *z*; C: 1–*x*, *y*, 0.5–*z*; D: 1–*x*, 1+*y*, 0.5–*z*; E: 0.5+*x*, 0.5+*y*, *z*).

distances ranging from 2.617 to 2.878 Å, which further link its symmetric part through two *syn,syn*-μ_2:η^1:η^1-carboxyl groups from two nda^{2-} ligands between Ag4 and Ag4C (C: 1–*x*, *y*, 0.5–*z*) to construct Ag_{10} units (Fig. 6) with 10 silver atoms almost locating at one plane. Strong Ag···Ag interactions are also found within Ag1A···Ag5A of 2.8616(10) Å and Ag4···Ag4C of 2.869 Å, significantly shorter than the Van der Waals contact distance (3.44 Å), and slightly shorter than the Ag···Ag contact distance in metallic silver (2.88 Å), indicating the existence of argentophilicity can promote the aggregation of silver centers [32,33]. In addition, other Ag···Ag weak interactions show the distances of about 3.1217(9)–3.7397(9) Å.

From Fig. 7a, down the *c*-axis direction, every decanuclear unit is connected to two other decanuclear units by three nda^{2-} and additional connections to other four decanuclear units by six μ_3-dmt ligands. Besides, it is observed that every decanuclear unit is further connected to two other decanuclear units by two nda^{2-} ligands, respectively (Fig. 7c). From the view of topology, ignoring the roles of some nda^{2-} ligands, each decanuclear unit may be treated as an 8-connected node, each dmt ligand being looked as three-connected node and nda^{2-} ligand along the *c*-axis direction being the linker, the overall structure can be described as 2-nodal (3,8)-connected with the point symbol of $\{4^3\}_2\{4^6.6^{18}.8^4\}$, which is a rare topology with **tfz-d** type (Fig. 7d), resembling that of $C_{53}H_{41.5}CoN_7O_{9.5}Zn_2$ [17]. In this case, the infinitely trinuclear zinc secondary building units and $[Co(4\text{-cpdpm})_3]$ ($4\text{-cpdpm})_3$=5-(4-carboxyl-phenyl)-4,6-dipyrrinato) metalloligands are both considered as hexagonal and trigonal nodes, which obtained the first (3,8)-connected **tfz-d** type. Additionally, in compound **2**, four kinds of N–H···O hydrogen-bonding interactions (see Table S2) are observed between the amino-N atoms of dmt and the carboxylic-O atoms of nda^{2-}, as well as a strong $\pi\cdots\pi$ packing interaction from triazine ring and naphthyl ring between dmt and nda^{2-} with the vertical plane–plane distance of 3.38 Å, the

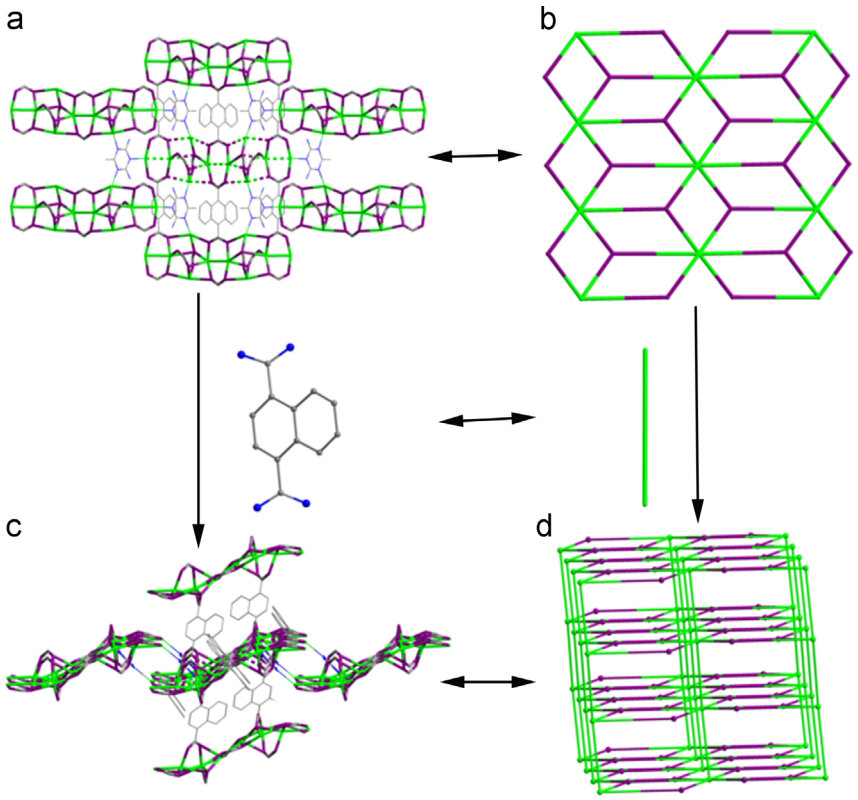

Fig. 7. Topology of compound **2**. The structure viewed perpendicular to *c* axis (a). Schematic representations of compound **2** (b) and (d). The 3D network viewed perpendicular to *b* axis (c).

centroid–centroid distance of about 3.39 Å, to increase the stability of the 3D network.

To the best of knowledge, though several cases involving in decanuclear Ag(I) compound have been reported [34–37], all compounds exhibit only discrete clusters. For example, the decanuclear cluster $[Ag_{10}(dcapp)_4]\cdot 2(OH)\cdot 12H_2O$ (H_2dcapp=2,6-dicarboxamido-2-pyridylpyridine) exhibits crownlike architecture, in which the silver atoms are arranged in two sides Ag_4 tetrahedrons and a central Ag_6 octahedron through Ag···Ag interactions [35]. However, the metal topology in **2** is different from that of the above compound, in that six silver atoms in the middle form almost planar configuration while two sides silver atoms show Ag_4 trigonal planar geometries. The compound **2** reveals the first example that decanuclear silver units as secondary building units connected by the ligands dmt and nda^{2-} to form 3D network, which firstly exhibits dimensionality change from 0D decanuclear dicrete molecules into 3D network.

3.4. Magnetic property of 1

The temperature dependence $\chi_m T$ and χ_m of **1** are shown in Fig. 8 (from 300 K to 2 K). The $\chi_m T$ value is 4.43 $cm^3\ mol^{-1}\ K$ at 300 K, close to that expected value 4.38 $cm^3\ mol^{-1}\ K$ of one magnetically isolated spin Mn(II) ions ($S_{Mn}=5/2$, $g=2.0$). Upon cooling, the $\chi_m T$ value steadily decreases to reach the value of 3.36 $cm^3\ mol^{-1}\ K$ at 50 K, and then the $\chi_m T$ value rapidly drops to 0.25 $cm^3\ mol^{-1}\ K$ at 2 K upon further cooling, which show antiferromagnetic behavior between Mn(II) ions. The molar susceptibilities of **1** obey the Curie–Weiss law in the temperature 300–25 K, giving $C=4.76\ cm^3\ K\ mol^{-1}$ and $\theta=-23.76$ K. Although compound **1** manifests 3D network consisting of 1D chain by nda^{2-}, the adjacent chains are separated by the long ligand, and therefore interchain magnetic interactions may be assumed

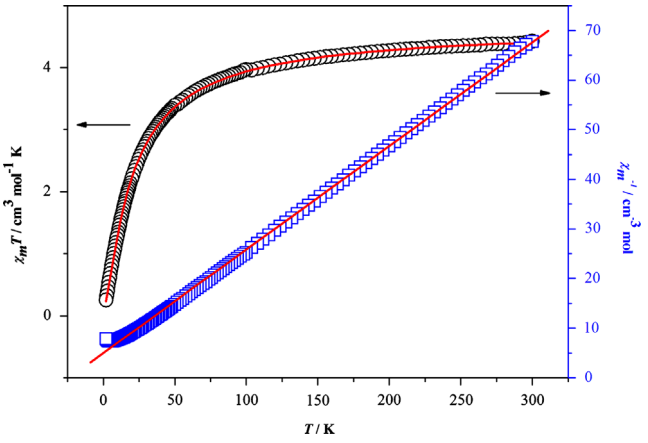

Fig. 8. The $\chi_m T$ *vs. T* and χ_m^{-1} *vs. T* plots of **1** in the range 2–300 K at 1 kG. The solid line is the best-fit.

neglectable. Here, we try to use a 1D Mn(II) chain model to fit the magnetic data: [38–40]

$$\chi_{chain} = \frac{Ng^2\beta^2 S(S+1)}{3kT}\frac{1+u}{1-u}$$

where

$$u = \coth\left[\frac{JS(S+1)}{kT}\right] - \left[\frac{kT}{JS(S+1)}\right]$$

Here, N, β and k represent Avogadro's number, Bohr's magneton and Boltzmann's constant.

In addition, taking into account other magnetic interactions between the 1D Mn(II) chains, the parameter zj' was added as

followed:

$$\chi_m = \frac{\chi_{chain}}{1-(2zj'/Ng^2\beta^2)\chi_{chain}}$$

The best fitting gave g=2.07, $J=-1.42$ (1) cm^{-1}, $zj'=-0.73$ (2) cm^{-1} and $R=3\times10^{-4}$ (the agreement factor defined as $(R=\Sigma[(\chi_mT)_{calcd}-(\chi_mT)_{obsd}]^2/\Sigma[(\chi_mT)_{obsd}]^2)$, which suggests the weak antiferromagnetic coupling interaction between Mn(II) ions. Within the chain, there are two sets of magnetic exchange pathways: one consists of two *syn*, *syn*-μ_2-carboxylate bridges, showing the antiferromagnetic interactions [41,42]. The other is made up of μ_2-O bridges, in which the Mn–O–Mn angles are 107.7 °, slightly bigger than the literature reported that the antiferromagnetic interations are indicated by the Mn–O–Mn angles in the range of 103.5–104.0 ° [43]. The magnetization is 1.36 Nβ at 5 T, far smaller than the expected saturation value 5 Nβ for one isolated Mn(II) ($S=5/2$, $g=2$) (Fig. S2).

3.5. Photoluminescent property of **2**

Vast Ag(I) complexes are known to emit photoluminescence at low temperature [44], and only a few Ag(I) complexes display photoluminescence at room temperature [45,46]. The solid-state emission spectra of complex **2** at room temperature are shown (Fig. S6). It can be seen that the maximum of the emission band of **2** is located at 472 nm ($\lambda_{ex}=394$ nm). The emission band of free dmt ($\lambda_{em}=390$ nm, $\lambda_{ex}=300$ nm) can be assigned to the $\pi^*-\pi$ transition [15], which is slightly stronger compared to that of π^*-n transition of the H_2nda ligand ($\lambda_{em}=480$ nm, $\lambda_{ex}=300$ nm) [13]. The emission band of **2** originates from the ligand-to-metal charge-transfer bands (LMCT) [47–52], mixed with metal-centered (d–s/d–p) transitions [53–56]. The shifted emission and enhancement of photoluminescence of **2** is attributed to the ligand coordination to the metal center, which effectively increases the rigidity of the ligand and reduces the loss of energy by radiationless decay.

4. Conclusions

Based on dmt, H_2nda and different transition metal salts, we have synthesized and structurally characterized two novel coordination complexes. The feature of the compound **1** is that it exhibits a 3D network including 1D linear chain $\{MnO(CO_2)_2\}_n$ connected by the ligand nda^{2-} with four-connected uninodal diamond-like topology. The compound 2 constructs the first 3D network by the decanuclear silver as secondary building units connected by the nda^{2-} and dmt ligands with a rare 2-nodal (3,8)-connected tfz–d topology ($\{4^3\}_2\{4^6.6^{18}.8^4\}$). Furthermore, compound **1** shows antiferromagnetic coupling between the neighboring Mn(II) ions and compound **2** displays solid-state fluorescent emissions at about 472 nm ($\lambda_{ex}=394$ nm).

Acknowledgments

This research is supported by the National Science Foundation of China (21271025), the National Science Foundation of the Education Department of Henan Province (2011A150004, 12B150004), the Department of Science and Technology of Henan Province (122102210174), the State Key Laboratory of Structural Chemistry (20110008).

Appendix A. Supporting information

Supplementary data associated with this article can be found in the online version at http://dx.doi.org/10.1016/j.jssc.2013.05.028.

References

[1] A.F.R. Kilpatrick, S.V. Kulangara, M.G. Cushion, R. Duchateau, P. Mountford, Dalton Trans. 39 (2010) 3653–3664.
[2] B.Y. Li, F. Yang, G.H. Li, D. Liu, Q. Zhou, Z. Shi, S.H. Feng, Cryst. Growth Des. 11 (2011) 1475–1485.
[3] T.K. Maji, S. Sain, G. Mostafa, T.H. Lu, J. Ribas, M. Monfort, N.R. Chaudhuri, Inorg. Chem. 42 (2003) 709–716.
[4] I. Ara, J. Forniés, J. Gómez, E. Lalinde, R.I. Merino, M.T. Moreno, Inorg. Chem. Commun. 2 (1999) 62–65.
[5] X. Liu, G.C. Guo, M.L. Fu, X.H. Liu, M.S. Wang, J.S. Huang, Inorg. Chem. 45 (2006) 3679–3685.
[6] S. Hu, F.Y. Yu, P. Zhang, A.J. Zhou, Eur. J. Inorg. Chem. (2012) 3669–3673.
[7] Q.G. Zhai, C.Z. Lu, X.Y. Wu, S.R. Batten, Cryst. Growth Des. 7 (2007) 2332–2342.
[8] F.J. Martínez Casado, O. Fabelo, J.A. Rodrígue-Velamazán, M. Ramos Riesos, J.A. Rodríguez Cheda, A. Labrador, C. Rodríguez-Blanco, J. Campo, V. Sánchez-Alarcos, H. Müller, Cryst. Growth Des. 11 (2011) 4080–4089.
[9] J.C. Jin, Y.Y. Wang, W.H. Zhang, A.S. Lermontonv, E.K. Lermontovaa, Q.Z. Shia, Dalton. Trans. (2009) 10181–10191.
[11] C. Sterb, C. Ritchie, D.L. Long, P. Kögerler, L. Cronin, Angew. Chem. Int. Ed. 46 (2007) 7579–7582.
[12] P. Lightfoot, A. Snedden, J. Chem. Soc., Dalton Trans. (1999) 3549–3551.
[13] D. Sun, Y.H. Li, F.J. Liu, H.J. Hao, R.B. Huang, L.S. Zheng, Inorg. Chem. Commun. 14 (2011) 1871–1875.
[14] H.J. Hao, D. Sun, Y.H. Li, F.J. Liu, R.B. Huang, L.S. Zheng, Cryst. Growth Des. 11 (2011) 3564–3578.
[15] D. Sun, Y.H. Li, H.J. Hao, F.J. Liu, Y. Zhao, R.B. Huang, L.S. Zheng, CrystEngComm 13 (2011) 6431–6441.
[16] D. Sun, H.J. Hao, F.J. Liu, H.F. Su, R.B. Huang, L.S. Zheng, CrystEngComm 14 (2012) 480–487.
[17] S.J. Garbay, J.R. Stork, Z.Q. Wang, S.M. Cohen, S.G. Telfer, Chem. Commun. (2007) 4881–4883.
[18] G.M. Seldrick, SHELXS-97, Program for X-ray Crystal Structure Solution, University of Göttingen, Göttingen, Germany, 1997.
[19] G.M. Sheldrick, SHELXL-97, Program for X-ray Crystal Structure Refinement, University of Göttingen, Göttingen, Germany, 1997.
[20] X.J. Zheng, L.C. Li, S. Gao, L.P. Jin, Polyhedron 23 (2004) 1257–1262.
[21] T.C. Stamatatos, K.A. Abboud, W. Wernsdorfer, G. Christou, Angew. Chem. Int. Ed. 47 (2008) 6694–6698.
[22] R.D. Poulsen, A. Bentien, M. Chevalier, B.B. Lversen, J. Am. Chem. Soc. 127 (2005) 9156–9166.
[23] T. Ladrak, S. Smulders, O. Roubeau, S.J. Teat, P. Gamez, J. Reedijk, Eur. J. Inorg. Chem. (2010) 3804–3812.
[24] N.L. Rosi, J. Kim, M. Eddaoudi, B.L. Chen, M. O'Keeffe, O.M. Yaghi, J. Am. Chem. Soc. 127 (2005) 1504–1518.
[25] G.H. Xu, X.G. Zhang, P. Guo, C.L. Pan, H.J. Zhang, J. Am. Chem. Soc. 132 (2010) 3656–3657.
[26] Y.W. Li, H. Ma, Y.Q. Chen, K.H. He, Z.X. Li, X.H. Bu, Cryst. Growth Des. 12 (2012) 189–196.
[27] H.J. Hao, D. Sun, F.J. Liu, R.B. Huang, L.S. Zheng, Cryst. Growth Des. 11 (2011) 5475–5482.
[28] L. Feng, Z.X. Chen, T.B. Liao, P. Li, Y. Jia, X.F. Liu, Y.T. Yang, Y.M. Zhou, Cryst. Growth Des. 9 (2009) 1505–1510.
[29] T.K. Maji, W. Kaneko, M. Ohba, S. Kitagawa, Chem. Commun. (2005) 4613–4615.
[30] Z.L. Liao, G.D. Li, M.H. Bi, J.S. Chen, Inorg. Chem. 47 (2008) 4844–4853.
[31] C.S. Liu, J.J. Wang, Z. Chang, L.F. Yan, T.L. Hu, Z. Anorg. Allg. Chem. 635 (2009) 523–529.
[32] D. Sun, G.G. Luo, N. Zhang, R.B. Huang, L.S. Zheng, Chem. Commun. 47 (2011) 1461–1463.
[33] P. Nockemann, B. Thijs, K.V. Hecke, L.V. Meervelt, K. Binnemans, Cryst. Growth Des. 8 (2008) 1353–1363.
[34] X.L. Zhao, Q.M. Wang, T.C.W. Mak, Inorg. Chem. 42 (2003) 7872–7876.
[35] H.W. Hou, Y.L Wei, Y.L. Song, L.W. Mi, M.S. Tang, L.K. Li, Y.T. Fan, Angew. Chem. Int. Ed. 44 (2005) 6067–6074.
[36] D.J. Eisler, R.J. Puddephatt, Inorg. Chem. 44 (2005) 4666–4678.
[37] J.J. Henkelis, C.A. Kilner, Chem. Commun. 47 (2011) 5187–5189.
[38] M.E. Fisher, Am. J. Phys 32 (1964) 343–346.
[39] Y.Q. Wei, Y.F. Yu, K.C. Wu, Cryst. Growth Des. 8 (2008) 2087–2089.
[40] H.R. Wen, C.F. Wang, Y. Song, J.L. Zuo, X. You, Inorg. Chem. 44 (2005) 9039–9045.
[41] M. Chen, S.S. Chen, T. Okamura, Z. Su, M.S. Chen, Y. Zhao, W.Y. Sun, Cryst. Growth Des. 11 (2011) 1901–1912.
[42] R.H. Wang, E.Q. Gao, M.C. Hong, S. Gao, J.H. Luo, Z.Z. Lin, Inorg. Chem. 42 (2003) 5486–5488.
[43] C. Desroches, G. Pilet, S.A. Borshch, S. Parola, D. Luneau, Inorg. Chem. 44 (2005) 9112–9120.
[44] C. Seward, J. Chan, D. Song, S. Wang, Inorg. Chem. 42 (2003) 1112–1120.
[45] D. Sun, R. Cao, J. Weng, M. Hong, Y. Liang, J. Chem. Soc., Dalton Trans. (2002) 291–292.
[46] D. Sun, G.G. Luo, N. Zhang, Q.J. Xu, R.B. Huang, L.S. Zheng, Polyhedron 29 (2010) 1243–1250.
[47] J. Tao, J.X. Shi, M.L. Tong, X.X. Zhang, X.M. Chen, Inorg. Chem. 40 (2001) 6328–6330.
[48] J. Zhang, W. Lin, Z.F. Chen, R.G. Xiong, B.F. Abrahams, H.K. Fun, J. Chem. Soc. Dalton Trans. (2001) 1806–1807.

[49] J.C. Dai, X.T. Wu, Z.Y. Fu, C.P. Cui, S.M. Wu, W.X. Du, L.M. Wu, H.H. Zhang, R. Q. Sun, Inorg. Chem. 41 (2002) 1391–1396.
[50] W. Chen, J.Y. Wang, C. Chen, Q. Yue, H.M. Yuan, J.S. Chen, S.N. Wang, Inorg. Chem. 42 (2003) 944–946.
[51] L.Y. Zhang, G.F. Liu, S.L. Zheng, B.H Ye, X.M. Zhang, X.M. Chen, Eur. J. Inorg. Chem. (2003) 2965–2971.
[52] S.L. Zheng, J.H. Yang, X.L. Yu, X.M. Chen, W.T. Wong, Inorg. Chem. 43 (2004) 830–838.
[53] A. Barbieri, G. Accorsi, N. Armaroli, Chem. Commun. (2008) 2185–2193.
[54] V.W.W. Yam, K.K.W. Lo, Chem. Soc. Rev. 28 (1999) 323–334.
[55] D. Sun, N. Zhang, R.B. Huang, L.S. Zheng, Cryst. Growth Des. 10 (2010) 3699–3709.
[56] S.R. Hettiarachchi, B.K. Schaefer, R.L. Yson, R.J. Staples, R. Herbast-Irmer, H.H. Patterson, Inorg. Chem. 46 (2007) 6997–7004.